

## CHANDRA TEMPERATURE MAP OF A754 AND CONSTRAINTS ON THERMAL CONDUCTION

M. MARKEVITCH,<sup>1</sup> P. MAZZOTTA,<sup>2</sup> A. VIKHLININ,<sup>1,3</sup> D. BURKE,<sup>1</sup> Y. BUTT,<sup>1</sup> L. DAVID,<sup>1</sup> H. DONNELLY,<sup>1</sup>  
W. R. FORMAN,<sup>1</sup> D. HARRIS,<sup>1</sup> D.-W. KIM,<sup>1</sup> S. VIRANI,<sup>1</sup> AND J. VRTILEK<sup>1</sup>

Received 2003 January 17; accepted 2003 February 7; published 2003 February 20

### ABSTRACT

We use *Chandra* data to derive a detailed gas temperature map of the nearby, hot, merging galaxy cluster A754. Combined with the X-ray and optical images, the map reveals a more complex merger geometry than previously thought, possibly involving more than two subclusters or a cool gas cloud sloshing independently from its former host subcluster. In the cluster central region, we detect spatial variations of the gas temperature on all linear scales, from 100 kpc (the map resolution) and up, which likely remain from a merger shock passage. These variations are used to derive an upper limit on effective thermal conductivity on a 100 kpc scale, which is at least an order of magnitude lower than the Spitzer value. This constraint pertains to the bulk of the intracluster gas, as compared to the previously reported estimates for cold fronts (which are rather peculiar sites). If the conductivity in a tangled magnetic field is at the recently predicted higher values (i.e., about  $\frac{1}{5}$  Spitzer), the observed suppression can be achieved, for example, if the intracluster gas consists of magnetically isolated domains.

*Subject headings:* conduction — galaxies: clusters: individual (A754) — intergalactic medium — magnetic fields — X-rays: galaxies: clusters

*On-line material:* color figures

### 1. INTRODUCTION

Since the nondetection by *XMM* and *Chandra* of the expected quantities of cool gas in cluster central regions (Peterson et al. 2001 and later works), there has been a renewed interest in heat conduction as a possible mechanism to offset radiative cooling (e.g., Narayan & Medvedev 2001; Gruzinov 2002; Fabian, Voigt, & Morris 2002). Detailed analyses of several cooling flow clusters (Voigt et al. 2002; Zakamska & Narayan 2003) show that heat inflow from the outer regions may indeed be sufficient over most of the cooling region, but only if the conductivity,  $\kappa$ , is not lower than  $\kappa_S/3$ , where  $\kappa_S$  is the Spitzer (1962) value. Such high conduction would have other important effects, e.g., erasing the cluster-scale temperature gradients (e.g., David, Hughes, & Tucker 1992) and causing significant heat loss into the intercluster space (Loeb 2002).

The conductivity of the cluster plasma should be reduced by the magnetic fields; however, theoretical estimates for such a reduction have not yet converged (see §3.2 for details). On the observational side, David et al. (1992) derived a lower limit of  $\kappa > \kappa_S/10$  for the Coma Cluster. However, recent higher resolution data revealed temperature variations in the cluster region that those authors assumed isothermal (e.g., Neumann et al. 2003), which may weaken their constraint. The only cluster-scale results derived so far using the high-resolution data were for the conduction across cold fronts. Etori & Fabian (2000) pointed out that the temperature jumps across the fronts in A2142 observed by *Chandra* (Markevitch et al. 2000) imply  $\kappa < \kappa_S/250$ . Although one can argue that as the cold front moves, the temperature gradient may be continually sharpened because of stripping of the heated boundary layer, their conclusion should be correct. As shown by Vikhlinin, Markevitch, & Murray (2001c) for A3667, there is no such boundary layer,

and the gas density discontinuity at the front is very sharp —much narrower than the electron mean free path, indicating that diffusion and conduction across the front are indeed suppressed. The likely reason is a layer of the magnetic field parallel to the front, which can form as the gas flows around the front and straightens the tangled field lines (Vikhlinin, Markevitch, & Murray 2001b). Another place where conductivity was estimated is the boundary between the hot cluster gas and two cool, galaxy-size dense gas clouds in Coma (Vikhlinin et al. 2001a). For these clouds to survive, conduction across their boundaries should be reduced by a factor of 30–100.

Those measurements probe rather peculiar sites in clusters, i.e., boundaries between different gas phases that are expected to have disjoint magnetic fields and so be thermally isolated. As we will show below, an estimate that is more representative of the bulk of the gas can be obtained from the temperature maps of hot merging clusters, such as A754.

Previous optical and X-ray studies of A754 —a rich cluster at  $z = 0.054$ —show that it is the prototype of a major merger. It has a complex galaxy distribution, X-ray morphology, and gas temperature structure (Fabricant et al. 1986; Bird 1994; Slezak, Durret, & Gerbal 1994; Zabludoff & Zaritsky 1995; Henry & Briel 1995; Henriksen & Markevitch 1996, hereafter HM96). It also exhibits a radio halo (Kassim et al. 2001). In this Letter, we use *Chandra* data to derive a detailed gas temperature map for A754. In § 3.1, we discuss the merger details revealed by the new data. In § 3.2, our temperature map is used for an estimate of the thermal conductivity of the cluster gas. At this redshift,  $1'' = 1.13$  kpc for our assumed  $H_0 = 65 h_{65} \text{ km s}^{-1} \text{ Mpc}^{-1}$ .

### 2. DATA ANALYSIS

A754 was observed by *Chandra* in 1999 October using ACIS-I<sup>4</sup> for a clean exposure of 39 ks. Our analysis procedure, briefly outlined below, follows that in Markevitch et al. (2000) and

<sup>1</sup> Harvard-Smithsonian Center for Astrophysics, 60 Garden Street, Cambridge, MA 02138; maxim@head-cfa.harvard.edu.

<sup>2</sup> University of Durham, Department of Physics, South Road, Durham DH1 3LE, UK; pasquale.mazzotta@durham.ac.uk.

<sup>3</sup> Space Research Institute (IKI), Russian Academy of Sciences, Profsoyuznaya 84/32, Moscow 117810, Russia; alexey@hea.iki.rssi.ru.

<sup>4</sup> *Chandra X-Ray Observatory* Guide available at <http://cxc.harvard.edu/proposer/POG>, “Observatory Guide,” “ACIS.”

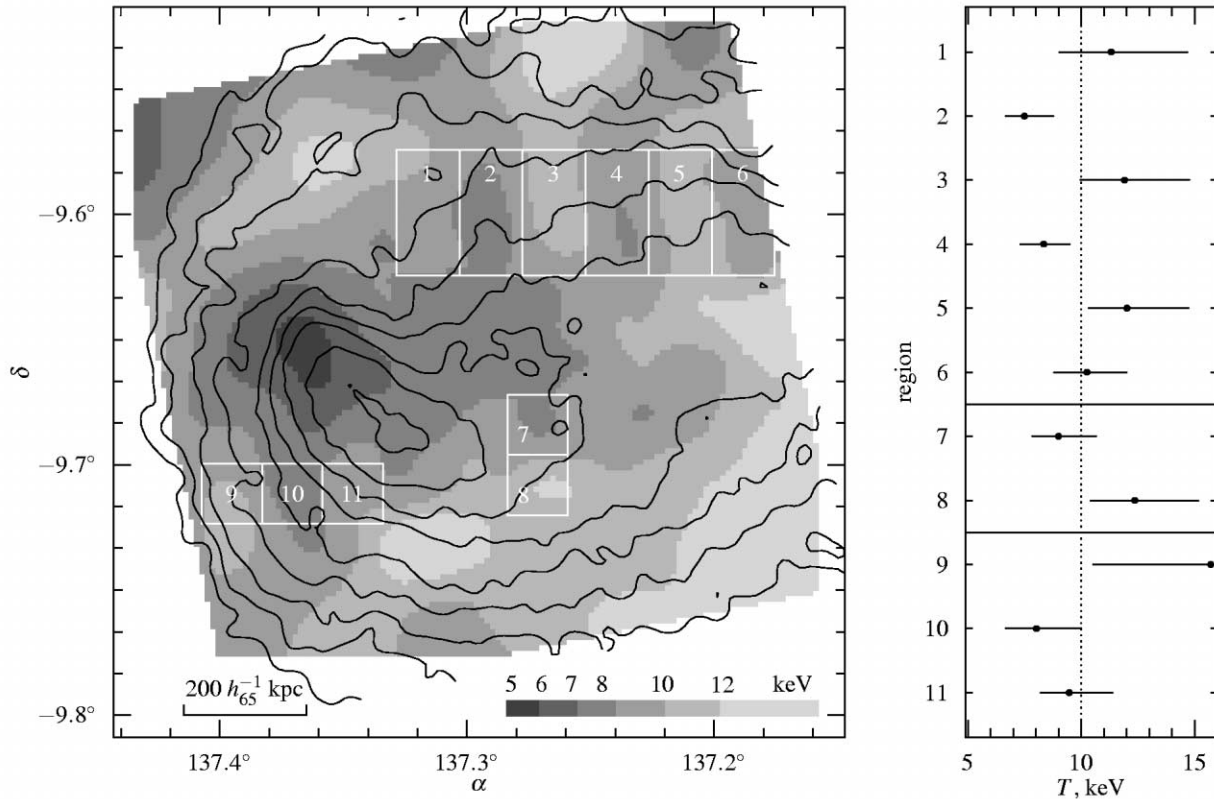


FIG. 1.—Projected temperature map of A754 (gray scale) overlaid on the ACIS 0.8–5 keV image (contours, spaced by  $\sqrt{2}$ ). Point sources are excluded. The map is adaptively smoothed (as part of the fitting procedure) by a Gaussian with  $\sigma$  between 25" and 55"; the image is smoothed with  $\sigma$  between 10" and 14". In most areas, different colors correspond to significantly different temperatures. Direct temperature fits for regions shown by white rectangles are given in the right panel (errors are 90%). The vertical dotted line shows the cluster average temperature. The step of the rectangles is 100 kpc. [See the electronic edition of the *Journal* for a color version of this figure.]

Markevitch & Vikhlinin (2001) with a few updates. For background subtraction, we used the ACIS blank-sky data set normalized by the ratio of the 10–12 keV rates in the data and the background files (see Markevitch et al. 2003); this normalization was within 1% of their exposure ratio. From the *ROSAT* All-Sky Survey (Snowden et al. 1997), there is no soft Galactic excess at the cluster position, so no additional background modeling was necessary. The detector low-energy response was corrected for the secular change of the ACIS quantum efficiency (Plucinsky et al. 2003). All point sources were masked out.

A single-temperature fit to the spectrum for the whole cluster (as far as we could reach,  $r = 9' = 0.6 h_{65}^{-1}$  Mpc) gives  $T_e = 10.0 \pm 0.3$  keV and a metal abundance of  $0.30 \pm 0.05$  (relative to Anders & Grevesse 1989) at the 90% confidence level. This temperature is somewhat higher than the *ASCA* value of 8.5–9.0 keV (HM96); however, *ASCA* covered more of this highly nonisothermal cluster. The absorption column, if fitted as a free parameter, is in good agreement with the Galactic value of  $N_H = 4.36 \times 10^{20} \text{ cm}^{-2}$  and therefore was fixed.

To derive a temperature map, we extracted cluster images in seven energy bands between 0.8 and 9.0 keV, excluding the interval 1.8–2.2 keV because of the poor calibration and the interval 7.4–7.6 keV containing a bright fluorescent background line. These images were adaptively smoothed (identically in all energy bands). Then in each image pixel, the seven flux values were fitted by a thermal model with fixed  $N_H$  and abundances. The result is shown in Figure 1.

### 3. DISCUSSION

The large-scale temperature structure is in broad agreement with earlier *ROSAT* and *ASCA* results (Henry & Briel 1995; HM96). The new map offers a much more detailed look into this interesting cluster. Of note are a large hot area to the south and southwest (already seen in the earlier data), cool gas at the northeast tip of the elongated central bright body, and numerous small-scale temperature variations. Most of these variations are statistically significant; to illustrate this, we extracted and fitted the real spectra for several less convincing features (right panel in Fig. 1). There is also a curious wavy structure in both the X-ray brightness and the temperature map (in the general area of regions 1–6 in Fig. 1), whose origin we find hard to explain.

#### 3.1. Merger Geometry

HM96 proposed that A754 is an off-center merger, and Roettiger, Stone, & Mushotzky (1998) succeeded in reproducing the general large-scale X-ray structure in hydrodynamic simulations. In Figure 2, which overlays X-ray and optical images, one can discern two main galaxy concentrations, one around the western brightest galaxy and another just south of the X-ray brightness peak (e.g., Fabricant et al. 1986; Zabludoff & Zaritsky 1995). While the western X-ray extension (not completely covered by our data, but see, e.g., Henry & Briel 1995) is associated with the western galaxy concentration, the second galaxy subcluster is offset from its presumed X-ray counterpart,

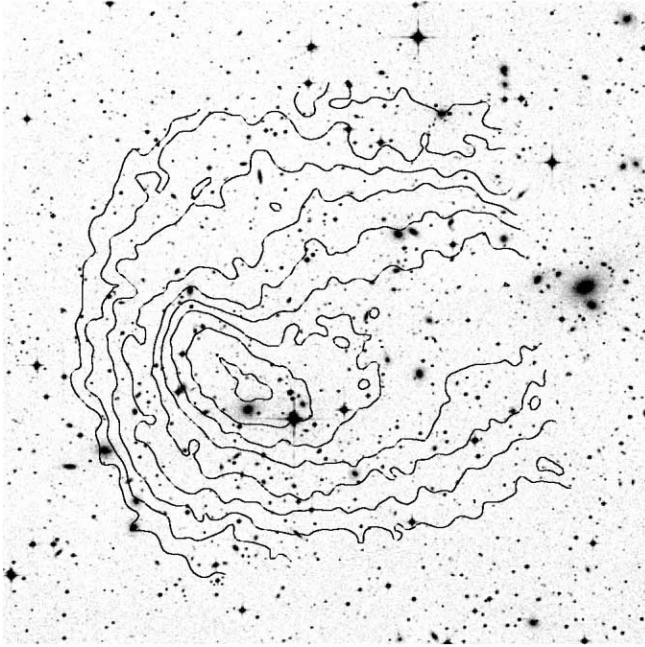


FIG. 2.—*Chandra* X-ray brightness contours (same as in Fig. 1) overlaid on the Palomar Digitized Sky Survey optical image. [See the electronic edition of the *Journal* for a color version of this figure.]

the bright elongated core (Zabludoff & Zaritsky 1995). In the Roettiger et al. (1998) simulations, this elongation and offset are caused by the ram pressure exerted from the southeast by the gas that used to belong to the western galaxy subcluster (which is now moving farther to the northwest).

However, the *Chandra* data complicate this picture by revealing interesting structure within the elongated gas core. There is a steep X-ray brightness drop-off at the northern tip of the body (Figs. 1 and 2) that, although not as sharp and regular-shaped as some cold fronts (e.g., Vikhlinin et al. 2001b), indicates a similar moving interface. The elongated cloud apparently moves to the north (in projection) from the big galaxy concentration, not being swept away by ram pressure from the south but as if dragged along by another subcluster. The cold region at the nose of the elongated body appears to be the former core of that subcluster. However, it does not coincide with any large galaxy concentration (although there is a possible small group there, which alone would not be considered statistically significant). Alternatively, in the course of the merger, the elongated cloud may have completely decoupled from its former dark matter host and is now “sloshing” independently. Such a state would be very short-lived because a moving gas cloud without the dark matter gravity support is quickly destroyed by gasdynamic instabilities.

The coolest spot does not coincide with the gas density peak, so apparently it is not in pressure equilibrium with the rest of the elongated core. Such a transient state may arise, for example, if the cool core travels down the strong ambient pressure gradient faster than its internal sound speed. Its northern tip may then expand too fast for the internal pressure to equalize. It is also possible that complex projection effects are at play (e.g., the elongated core is a projection of two gas clouds).

We finally mention a brightness feature that looks like a bow shock leaving the merger site, first noted in the *ROSAT* image (Krivonos et al. 2003). It is located at the leftmost contour in

our figures (unfortunately, we cannot study this feature because of the limited coverage). It is consistent with the general merger picture proposed by Roettiger et al. (1998).

To conclude, simple scenarios cannot explain all the complex details in the new X-ray data on A754. However, the very complexity of the temperature map of this cluster can be used for an interesting physical estimate, as we show below.

### 3.2. Limit on Thermal Conduction

In a plasma with a temperature gradient  $\nabla T_e$  such that the gradient’s linear scale  $l_T \equiv T_e/|\nabla T_e| \gg \lambda_e$  (where  $\lambda_e$  is electron mean free path), the heat flux is given by  $q = -\kappa \nabla T_e$ . In the absence of magnetic fields and for typical cluster plasma parameters, the collisional conductivity is given by Spitzer (1962, p. 86):

$$\kappa_s = 1.31 n_e \lambda_e k (kT_e/m_e)^{1/2} \approx 7.1 \times 10^{13} \left( \frac{kT_e}{10 \text{ keV}} \right)^{5/2} \times \left( \frac{\ln \Lambda}{37.8} \right)^{-1} \text{ ergs s}^{-1} \text{ cm}^{-1} \text{ K}^{-1}, \quad (1)$$

where  $\ln \Lambda$  is the Coulomb logarithm. For magnetic fields expected in clusters ( $B > 0.1 \mu\text{G}$ ; Carilli & Taylor 2002), the electron and proton gyroradii are many orders of magnitude smaller than their Coulomb mean free paths. Therefore, conduction occurs predominantly along the magnetic field lines, and the effective conductivity is determined by the topology of the field. If the field is chaotic with a coherence scale  $l_B \gg \lambda_e$ , the conductivity on scales  $l_T \gg l_B$  is reduced by a factor of 3 (e.g., Sarazin 1988; Gruzinov 2002). If  $l_B \lesssim \lambda_e$  (which is likely the case; radio data suggest  $l_B \sim 5\text{--}30$  kpc [e.g., Carilli & Taylor 2002], while  $\lambda_e \approx 10\text{--}15$  kpc in the central region of A754), the effective conductivity is reduced because electrons have to travel a longer path along the tangled field lines to diffuse over a given distance. The reduction is of order  $(l_T/l_B)^2$  (e.g., Tribble 1989; note that  $\kappa$  becomes scale-dependent) but probably not more than a factor of 100 if one considers the physical origin of the tangled field (Rosner & Tucker 1989; Tao 1995). In addition, the conductivity *along* the field lines may be reduced by a factor of  $\sim 10$  (for  $l_B \sim \lambda_e$ ) by magnetic mirrors (Malyshekin & Kulsrud 2001). On the other hand, for certain spectra of the field fluctuations, diffusion across the field lines and divergence of the lines may boost the effective conductivity to within a factor of only  $\sim 5$  below  $\kappa_s$  (Narayan & Medvedev 2001). This requires a field tangled on a range of scales down to  $\sim l_B/100$ . We note that it is unclear whether such a field would be consistent with the observations of the  $\sim 10$  kpc coherent “patches” of polarization of the background radio sources (Carilli & Taylor 2002; Govoni 2001), if those measurements indeed probe typical intracluster fields. To summarize, the collisional thermal conductivity on 100 kpc scales is expected to be reduced by a factor of 3–100.

Our temperature map of A754 offers an interesting opportunity to put observational constraints on  $\kappa$ . All over the cluster, the temperature varies on linear scales starting from 100 kpc (the map resolution, limited by statistics) and up. This scale is so small that the temperature gradients should be erased very quickly if the conductivity is at the Spitzer value (eq. [1]). An

approximate expression for the conduction timescale  $t_{\text{cond}} \equiv -(d \ln T_e/dt)^{-1}$  can be found in, e.g., Sarazin (1988):

$$t_{\text{cond}} \sim kn_e l_T^2 / \kappa_S \approx 1.2 \times 10^7 \frac{n_e}{2 \times 10^{-3} \text{ cm}^{-3}} \times \left( \frac{l_T}{100 \text{ kpc}} \right)^2 \left( \frac{kT_e}{10 \text{ keV}} \right)^{-5/2} \text{ yr}, \quad (2)$$

where  $n_e$  is from Jones & Forman (1999);  $t_{\text{cond}} \propto h_{65}^{-3/2}$ . Note that  $l_T$  as defined above and determined from the map in Figure 1 would be greater than 100 kpc. However, we measure temperatures in projection, with a large column of gas at the mean cluster temperature on the line of sight, so the true temperature variations should be significantly stronger.<sup>5</sup> We therefore chose to use the apparent scale of the variations in the map as a realistic value of  $l_T$  for this estimate; this, along with the strong dependence of  $\kappa_S$  on  $T_e$ , are our greatest sources of uncertainty. We did not take into account mild saturation of the classical heat flux (for our  $\lambda_e$  and  $l_T$ , one expects  $\kappa \approx 0.7\kappa_S$ ; see Cowie & McKee 1977 and Sarazin 1988), which in reality should not occur because of the tangled fields. In any case, it would not affect the conclusion.

At the same time, we do see these temperature variations everywhere in the cluster, so they should have lived for at least as long as it takes for a merger shock and/or a disturbing subcluster (which presumably have created them via compression and gasdynamic instabilities) to travel across the central region of the cluster,  $L \geq 800$  kpc (approximately the size of our map). The sound speed in this region is a safe estimate of that shock's velocity, regardless of its Mach number, since this region now contains the postshock gas. This timescale is

$$t_{\text{age}} \geq \frac{L}{c_s} \approx 5 \times 10^8 \frac{L}{800 \text{ kpc}} \left( \frac{kT_e}{10 \text{ keV}} \right)^{-1/2} \text{ yr}; \quad (3)$$

$t_{\text{age}} \propto h_{65}^{-1}$ . A comparison of equations (2) and (3) shows that the conductivity is reduced by a factor

$$(\kappa/\kappa_S)^{-1} \sim t_{\text{age}}/t_{\text{cond}} \geq 40 h_{65}^{1/2}, \quad (4)$$

although we emphasize that, given all the uncertainties, this is only an order-of-magnitude estimate.

The limit in equation (4) is inconsistent with the upper end

<sup>5</sup> The average true distance between regions of different temperature in the map is also greater, but it is the size of each region, not the distance between them, that determines  $l_T$ .

of the theoretical range for  $\kappa$ . We note that the ‘‘local’’ conductivity considered by theorists can still be higher, if, for example, the intracluster medium consists of thermally isolated domains with self-contained field structure. Such domains of gas that belonged to different subclusters may survive if mixing during the merger is not very efficient, as is indeed suggested by the existence of cold fronts (Vikhlinin et al. 2001b; Narayan & Medvedev 2001).

Our upper limit on conduction appears to exclude it as a mechanism to offset cooling in the cluster cores (where one needs  $\kappa > \kappa_S/3$ ; see references in § 1). However, conduction in a denser, cooler core is likely to operate in a different regime; for example, there one expects  $\lambda_e \ll l_B$  compared to  $\lambda_e \sim l_B$  in the regions that we studied above. In addition, the central magnetic fields may have a different topology because of the competing effects of the radial cooling inflow (Bregman & David 1988; Soker & Sarazin 1990) and the radial infall of the subcluster pieces versus the widespread gas ‘‘sloshing’’ (Markevitch, Vikhlinin, & Forman 2003). This may result in a different reduction factor. Finally, we note that our limit in equation (4) as well as the cooling flow conduction estimates are relative to  $\kappa_S$ , which itself is much lower in the cool cores. Our *absolute* upper limit on conductivity is not necessarily lower than the *absolute* conductivity needed to compensate cooling. Thus, even if the reduction factor for the Spitzer conduction is the same everywhere in the cluster, we cannot exclude a sufficiently high heat influx into the cooling core that is due to a different physical process (and so has a different dependence on gas parameters), such as turbulence, for example.

#### 4. SUMMARY

We have derived a detailed temperature map of the prototypical merging cluster A754. Simple merger scenarios cannot reproduce the complex details revealed by the new data; either A754 is a three-body merger or the cool dense gas found in the cluster's bright elongated core has decoupled from its former subcluster host and is sloshing independently. We use the small-scale structure in the temperature map to derive the first constraint on thermal conductivity in the bulk of the gas in a cluster. The conductivity on scales  $\sim 100$  kpc appear reduced by at least an order of magnitude from the Spitzer value.

We are grateful to Professor T. Ohashi for an insightful question at a conference that led to the above conductivity estimate. Support was provided by NASA contract NAS8-39073, *Chandra* grant GO2-3164X, and the Smithsonian Institution.

#### REFERENCES

- Anders, E., & Grevesse, N. 1989, *Geochim. Cosmochim. Acta*, 53, 197  
 Bird, C. M. 1994, *AJ*, 107, 1637  
 Bregman, J. N., & David, L. P. 1988, *ApJ*, 326, 639  
 Carilli, C. L., & Taylor, G. B. 2002, *ARA&A*, 40, 319  
 Cowie, L. L., & McKee, C. F. 1977, *ApJ*, 211, 135  
 David, L. P., Hughes, J. P., & Tucker, W. H. 1992, *ApJ*, 394, 452  
 Ettori, S., & Fabian, A. 2000, *MNRAS*, 317, 57L  
 Fabian, A. C., Voigt, L. M., & Morris, R. G. 2002, *MNRAS*, 335, L71  
 Fabricant, D., Beers, T., Geller, M., Gorenstein, P., Huchra, J., & Kurtz, M. 1986, *ApJ*, 308, 530  
 Govoni, F. 2001, Ph.D. thesis, Univ. Bologna  
 Gruzinov, A. 2002, preprint (astro-ph/0203031)  
 Henriksen, M., & Markevitch, M. 1996, *ApJ*, 466, L79 (HM96)  
 Henry, J., & Briel, U. 1995, *ApJ*, 443, L9  
 Jones, C., & Forman, W. 1999, *ApJ*, 511, 65  
 Kassim, N. E., Clarke, T. E., Ensslin, T. A., Cohen, A. S., & Neumann, D. M. 2001, *ApJ*, 559, 785  
 Krivonos, R., Vikhlinin, A., Markevitch, M., & Pavlinsky, M. 2003, *Astron. Lett.*, submitted  
 Loeb, A. 2002, *NewA*, 7, 279  
 Malyshkin, L., & Kulsrud, R. 2001, *ApJ*, 549, 402  
 Markevitch, M., et al. 2003, *ApJ*, 583, 70  
 ———. 2000, *ApJ*, 541, 542  
 Markevitch, M., & Vikhlinin, A. 2001, *ApJ*, 563, 95  
 Markevitch, M., Vikhlinin, A., & Forman, W. R. 2003, in *Matter and Energy in Clusters of Galaxies*, ed. S. Bowyer & C.-Y. Hwang (San Francisco: ASP), in press (astro-ph/0208208)  
 Narayan, R., & Medvedev, M. V. 2001, *ApJ*, 562, L129  
 Neumann, D. M., Lumb, D. H., Pratt, G. W., & Briel, U.G. 2003, *A&A*, in press (astro-ph/0212432)  
 Peterson, J. R., et al. 2001, *A&A*, 365, L104

- Plucinsky, P. P., et al. 2003, Proc. SPIE, in press (astro-ph/0209161)
- Roettiger, K., Stone, J. M., & Mushotzky, R. F. 1998, ApJ, 493, 62
- Rosner, R., & Tucker, W. H. 1989, ApJ, 338, 761
- Sarazin, C. L. 1988, X-Ray Emission from Clusters of Galaxies (Cambridge: Cambridge Univ. Press)
- Slezak, E., Durret, F., & Gerbal, D. 1994, AJ, 108, 1996
- Snowden, S. L., et al. 1997, ApJ, 485, 125
- Soker, N., & Sarazin, C. L. 1990, ApJ, 348, 73
- Spitzer, J. 1962, Physics of Fully Ionized Gases (New York: Interscience)
- Tao, L. 1995, MNRAS, 275, 965
- Tribble, P. C. 1989, MNRAS, 238, 1247
- Vikhlinin, A., Markevitch, M., Forman, W., & Jones, C. 2001a, ApJ, 555, L87
- Vikhlinin, A., Markevitch, M., & Murray, S. S. 2001b, ApJ, 549, L47
- . 2001c, ApJ, 551, 160
- Voigt, L. M., Schmidt, R. W., Fabian, A. C., Allen, S. W., & Johnstone, R. M. 2002, MNRAS, 335, L7
- Zabludoff, A., & Zaritsky, D. 1995, ApJ, 447, L21
- Zakamska, N. L., & Narayan, R. 2003, ApJ, 582, 162